

## 2 THE GLOBAL INTEGRATED WATER MODEL WATERGAP 2.1

**Petra Döll<sup>\*</sup>, Joseph Alcamo, Thomas Henrichs, Frank Kaspar, Bernhard Lehner, Thomas Rösch, Stefan Siebert**

Center for Environmental Systems Research, University of Kassel, Germany

\*doell@usf.uni-kassel.de

### 2.1 Introduction

WaterGAP, a global model of water availability and water use, has been developed to assess the current water resources situation and to estimate the impact of global change on the problem of water scarcity (Döll et al., 1999; Alcamo et al., 2000). With a spatial resolution of 0.5°, the raster-based model is designed to simulate the characteristic macro-scale behavior of the terrestrial water cycle, including the human impact, and to take advantage of all pertinent information that is globally available. WaterGAP simulates the impact of demographic, socioeconomic and technological change on water use as well as the impact of climate change and variability on water availability and irrigation water use. To the author's knowledge, WaterGAP is the only global model that simulates both water availability – as surface runoff, groundwater recharge and river discharge – and water use in drainage basins (and not only in countries). Due to the newly developed 0.5° global drainage direction map DDM30 (Döll and Lehner, 2001), the analyzed drainage basins can be flexibly chosen, and the lateral transport of water can be adequately simulated.

WaterGAP consists of two main parts, the Global Hydrology Model and the Global Water Use Model. The Global Water Use Model itself is composed of four submodels, one for each of the water use sectors households, industry, irrigation and livestock. The Global Hydrology Model of WaterGAP 2.1 is calibrated against discharge measured at 724 gauging stations, the drainage areas of which cover about 50% of the global land area excluding Greenland and Antarctica, taking into account the reduction of natural discharge by consumptive water use.

WaterGAP 2 is presented by Döll et al. (2001) and Alcamo et al. (2001). Here, version 2.1 of WaterGAP, which was used for EuroWasser calculations, is described.

### 2.2 Model description

First, the spatial base data of WaterGAP 2.1, the land mask and the global drainage direction map DDM30, are described. Then, information on the applied climate information is given, as results of both the Global Hydrology Model and the Global Irrigation Model are strongly dependent on climate data. Finally, the Global Water Use Model and the Global Hydrology Model are presented.

### 2.2.1 Spatial base data

The computational grid of WaterGAP 2.1 consists of 66896 cells of size  $0.5^\circ$  by  $0.5^\circ$  and covers the global land area with the exception of Antarctica (IMAGE 2.2 land mask). It is based on the  $5'$  land mask of FAO's Soil Map of the World (FAO, 1995). A  $0.5^\circ$  cell that contains at least one  $5'$  land cell is defined as a computational cell. For each  $0.5^\circ$  cell, information on the fraction of land area and of freshwater area is available. The latter information was derived from a compilation of geographic information on lakes, reservoirs and wetlands at a resolution of  $1'$  (Lehner and Döll, 2001, see Section 2.2.4). Each of the computational cells belongs to a country and to one of 13 world regions, which are used for scenario generation.

The upstream/downstream relation among the grid cells, i.e. the drainage topology, is defined by the new global drainage direction map DDM30, which represents the drainage directions of surface water at a spatial resolution of  $0.5^\circ$  (Döll and Lehner, 2001). Each cell either drains into one of the eight neighboring cells, or into none if the cell represents an inland sink or a basin outlet to the ocean. Based on DDM30, the drainage basin of each cell can be determined, and the lateral transport of water can be simulated. DDM30 was generated by first upscaling two drainage direction maps (DDMs) at higher resolutions. The resulting map was then extensively corrected in an iterative manner by comparison against vectorized, high resolution river maps and other geographic information. Finally, it was co-referenced to the location of 935 gauging stations (provided by the Global Runoff Data Centre GRDC, Koblenz, Germany), which again involved manual corrections. DDM30 was validated against drainage basin areas from the literature, against the given upstream areas of the GRDC stations and against information from HYDRO1k (USGS, 2000), a data set based on a hydrologically-corrected 1-km digital elevation model which is thought to afford the best information on surface drainage currently available at the global scale. In the course of the validation, the quality of DDM30 was compared to three other  $0.5^\circ$  DDMs. The validation results show that DDM30 provides a more accurate representation of drainage directions and river network topology than the other  $30'$  DDMs.

### 2.2.2 Climate input

As climate input to WaterGAP 2.1, the data set by New et al. (2000) is used, which provides observed monthly values of precipitation, temperature, number of wet days per month, cloudiness and average daily sunshine hours, interpolated to a  $0.5^\circ$  by  $0.5^\circ$  grid. While for sunshine only the long-term average values of the period 1961-90 are given, the complete time series between 1901 and 1995 is available for the other variables.

In the Global Hydrology Model and the Global Irrigation Model, calculations are performed at a temporal resolution of one day. Synthetic daily precipitation values are generated from the monthly values by using the information on the number of wet days per

month, such that there are days with and without precipitation. The distribution of wet days within a month is modeled as a two-state, first-order Markov chain, the parameters of which were chosen according to Geng et al. (1986), who analyzed daily rainfall data from various locations around the globe. For each combination of the number of days in a month and the number of wet days, Markov chains were generated stochastically, and one sequence of wet and dry days was selected. Thus, in the model, each month with the same number of days and wet days has the same sequence of wet and dry days. The total monthly precipitation is distributed equally over all wet days of the month. The effect of snow is simulated by a simple degree-day algorithm.

Daily potential evapotranspiration  $E_{pot}$  is computed by WaterGAP according to Priestley and Taylor (1972), with the Priestley-Taylor coefficient  $\alpha = 1.26$  for areas with relative humidity of 60% or more and  $\alpha = 1.74$  for other areas, following the recommendation of Shuttleworth (1993). Net radiation  $R_n$  is computed as a function of the day of the year, latitude, sunshine hours and short-wave albedo following Shuttleworth (1993), except for the computation of the sunset hour angle which is better approximated by the CBM model of Forsythe et al. (1995). The computed net radiation and thus also the potential evapotranspiration is very sensitive to the use of either sunshine hours or cloudiness and global radiation provided by New et al. (2000); only when sunshine hours are used, the resulting potential evapotranspiration appears large enough. Daily values of sunshine hours and temperature are derived from the monthly values using cubic splines.

Future climate is simulated by changing monthly temperature and precipitation values only. Future temperature time series are computed by adding the difference between the future long-term average monthly value and the present-day long-term average value from climate model output (downscaled to  $0.5^\circ$ ) to the observed value of New et al. (2000). In the case of precipitation, the future climate model value as a ratio of the present-day value is multiplied by the observed value.

### 2.2.3 The Global Water Use Model

To the author's knowledge there are no published models of global water use and hence new model concepts were implemented in WaterGAP. The Global Water Use Model simulates both consumptive and withdrawal water use in the domestic, industrial, irrigation and livestock sectors. Withdrawal water use is the quantity of water taken from its natural location, while consumptive water use is the part of the withdrawn water that is lost by evapotranspiration. The difference between withdrawal and consumptive use is the return flow, the part of the withdrawn water that returns to either the surface water or the groundwater. The ratio of consumptive and withdrawal water use is called water use efficiency. In-situ water use (e.g. for navigation) is not taken into account in WaterGAP. Each sectoral water use is computed as a function of a water use intensity (e.g. per-capita domestic

water use of population with access to safe drinking water) and a driving force of water use (e.g. population with access to safe drinking water). In a scenario of future water use, both the water use intensities and the driving forces may differ from present-day conditions. Although all sectoral water uses are expected to vary at least to a certain degree with climate and the season of the year, only the strong seasonality and climate dependence of irrigation water use is simulated by the model. In WaterGAP 2.1, the main driving forces of water use are population in the domestic sector, national electricity production in the industry sector, area of irrigated land and climate in the irrigation sector and the number of livestock in the livestock sector. The base year for the computation of water use is 1995.

### *2.2.3.1 Domestic and industrial sectors*

Domestic and industrial water use is modeled based on country-specific estimates of domestic and industrial withdrawal and consumptive water use in 1995 (Shiklomanov, 2000). In the case of domestic water use, the country values are allocated to the WaterGAP grid cells within the country based on information of population density (Global Population Density Map at 5' x 5' Resolution of Tobler et al., 1995, as cited in van Woerden et al., 1995, scaled to 1995 country population), urban and rural population in each country (WRI, 1998) and fraction of inhabitants with access to safe drinking water in rural and urban areas (World Bank, 1996; WRI, 1998). The allocation steps are as follows:

- Rural population density of a country is assumed to be the same in each of the country's cells. If the such assumed rural population of a cell would be larger than the given total population, the surplus is distributed equally within the other country cells.
- The difference between the total population of each cell and the rural population is assumed to be urban population.
- The number of inhabitants in each cell that have access to safe drinking water is computed.
- Those inhabitants without access to safe drinking water are assumed to have a per capita domestic withdrawal water use of 7.3 m<sup>3</sup>/yr (20 l/d). The rest of the national water use is equally distributed to each inhabitant with access to safe drinking water. If the national data for a country list a per capita domestic withdrawal water use of less than 7.3 m<sup>3</sup>/yr, the listed value is assumed to be valid for each inhabitant of this country.
- The total domestic water use in a cell is computed as the sum of the water use by all the inhabitants without access to safe drinking water and those with access.

With respect to industrial water use, we neither have information on the partitioning between water use for cooling of power plants and for manufacturing nor on the specific locations of water users. Therefore, industrial water use is assumed to be distributed among the cells of a country in proportion to its urban population.

Two main concepts are used for modeling the future change in water intensity in the domestic and industrial sectors - *structural change* and *technological change*. Structural change in the domestic sector means that households in poorer countries first acquire more and more water-using appliances as their income increases. Eventually, the average household becomes saturated with water-using appliances, and as a result water use stabilizes. The consequence of these structural changes is that average water intensity of households [ $\text{m}^3/\text{cap}$ ] first sharply grows along with the growth per capita gross domestic product GDP, but eventually stabilizes as per capita GDP continues to grow. This trend is confirmed by data in Shiklomanov (2000). In WaterGAP 2.1 this process is represented by a sigmoid curve:

$$DSWI = DSWI_{\min} + DSWI_{\max} \cdot (1 - \exp(-\gamma_d \cdot GDP^2)) \quad (2.1)$$

where  $DSWI$  = domestic structural water intensity [ $\text{m}^3/\text{cap}$ ],  $GDP$  = per capita annual GDP and  $\gamma_d$  = curve parameter. Values of  $DSWI_{\min}$ ,  $DSWI_{\max}$ , and  $\gamma_d$  are calibrated for each of 26 world regions (grouping of countries) based on the trend of historical data by Shiklomanov (2000). Where adequate data are available, the parameters are calibrated to individual countries (USA, Canada, Japan and Germany).

In the industry sector, the concept of structural change of water use represents the change in water intensity [ $\text{m}^3/\text{MWh}$  produced electricity] with the change in the mix of water-using power plants and manufacturers within a particular country. In poorer countries the water intensity first sharply decreases (because these often rely on imported electricity) and then levels off with increasing national income (Shiklomanov, 2000). In richer regions the structural water intensity has either stabilized or has a very slight downward trend. Hence, structural changes in the industry sector are represented by a hyperbolic curve:

$$ISWI = \frac{1}{\gamma_i (GDP - GDP_{\min})} + ISWI_{\min} \quad (2.2)$$

where  $ISWI$  = industry structural water intensity [ $\text{m}^3/\text{MWh}$ ] and  $\gamma_i$  = curve parameter. The values of  $\gamma_i$  and the  $ISWI_{\min}$  are estimated for regions or countries as in the domestic sector.

The second main concept used to model water use in the domestic and industry sectors is technological change. While structural changes either increase or decrease water intensity, technological changes almost always lead to improvements in the efficiency of water use and a decrease in water intensity. Technological change is assumed to decrease water intensity by a certain rate, e.g. 1%/yr, resulting in a domestic and industrial water intensity that is a function of per capita GDP and time. To compute water withdrawals in the domestic sector, the domestic water intensity is multiplied by population. For industry water withdrawals, industrial water intensity is multiplied by electricity production. Here, electricity production is used as a surrogate of all driving forces in the sector. More realistically, both electricity

production and manufacturing output are the important driving forces of industrial water use, but it is not yet feasible to distinguish between these on the global level because of lack of data. Consequently, electricity generation is used because it is the dominant water user in the industry sector of most countries and because the magnitude of electricity production is a rough indicator of the magnitude of manufacturing output.

### 2.2.3.2 Irrigation sector

The Global Irrigation Model of WaterGAP 2.1 (Döll and Siebert, 2001) computes net and gross irrigation requirements, which reflect an optimal supply of water to irrigated plants; actual per hectare water uses may be lower due to restricted water availability. The *net irrigation requirement* refers to the part of the irrigation water that is evapotranspired by the plants (at the potential rate), while *gross irrigation requirement* refers to the total volume of water that is withdrawn from its source. The net and gross requirements are equivalent to *consumption* and *withdrawals* used elsewhere in this paper. The ratio of net over gross irrigation requirement is called irrigation water use efficiency. For scenario calculations this efficiency can be specified to increase with time because of technological changes in irrigation systems. This is parallel to the concept of *technological change* used above in the domestic and industry sectors.

The irrigation model uses a new digital global map of irrigated areas (Döll and Siebert, 2000; update for Latin America and Europe: Siebert and Döll, 2001) as the basis for the computations. The model simulates the cropping patterns, the growing seasons and the net and gross irrigation requirements, distinguishing two general crop types, rice and other crops. Rice is distinguished here because data are available for the extent of irrigated rice areas which are not available for other irrigated crops.

To compute gross irrigation requirements, first the cropping pattern for each cell with irrigated land is modeled using a rule-based system, incorporating data on total irrigated area, long-term average temperature, soil suitability for paddy rice in each cell, harvested area of irrigated rice in each country and cropping intensity in each of 19 world regions. Assuming a growing period of 150 days for both rice and other crops, the model determines for each grid-cell (i) whether only rice, only other crops or both are irrigated and (ii) whether, within one year, there are one or two growing seasons for rice and other crops (Döll and Siebert, 2001). Next, the optimal growing seasons are determined for each cell. The planting date within the growing season is computed for each crop and growing season by ranking each potential 150-day period within a year according to optimal temperature and precipitation conditions, which depend on the growing stage of the crop. The planting date is then defined by the highest ranked growing period; for those regions in which two consecutive growing periods are assumed, the combination of growing periods with the highest total number of ranking points is chosen.

The net irrigation requirement  $IR_{net}$  [mm/d] of rice and non-rice crops is computed for each day of the growing season as the difference between the crop-specific potential evapotranspiration  $k_c E_{pot}$  and the plant-available precipitation  $P_{avail}$ :

$$IR_{net} = k_c E_{pot} - P_{avail} \quad \text{if } k_c E_{pot} > P_{avail}$$

$$IR_{net} = 0 \quad \text{otherwise} \quad (2.3)$$

This approach is similar to the CROPWAT approach of Smith (1992). The plant-available precipitation is the fraction of effective precipitation (as rainfall and snowmelt) that is available to the crop and does not run off; it is computed following the USDA Soil Conservation Method as cited in Smith (1992). The net irrigation requirements are calculated by using the time series of climatic data described in section 2.2.2. The gross irrigation requirement is computed by taking into account regionally-varying irrigation field efficiencies ranging from 0.35 in South and East Asia to 0.7 in Canada, North Africa and Oceania (Döll and Siebert, 2001). These are rough estimates of project-level irrigation efficiencies.

As a test of the Global Irrigation Model, computed cropping patterns, growing seasons and irrigation requirements were compared with independent data. In most cases, model calculations come close to reality. For example, Roth (1993) estimated the net irrigation requirement on irrigated land in Germany to range from 80 to 110 mm/yr, as compared to the average of 112 mm/yr computed by the model. The best independent irrigation water use estimates are available for the US (data per county for 1995, Solley et al., 1998). A very good statistical agreement ( $R^2 = 0.98$ ) was found between calculated and actual average irrigation requirements (Döll and Siebert, 2001), despite the model's failure to correctly simulate the existing rice production area in California.

### 2.2.3.3 Livestock

In most parts of the world, livestock water use is very small compared to irrigation water use. In WaterGAP 2.1 the water withdrawals for livestock are assumed to be equal to the consumptive use and are computed by multiplying the number of livestock per grid cell (GlobalARC, 1996) by the livestock-specific water use per head and year. Ten livestock types are distinguished.

## 2.2.4 Global Hydrology Model

The Global Hydrology Model computes runoff and discharge at each grid cell by calculating the daily water balance of the cell. The vertical water balance is determined for both the land and the open water fraction (wetlands, lakes and reservoirs) of the cell. Total runoff from land is partitioned into fast surface/subsurface runoff and groundwater recharge and then transported laterally within the cell and to the downstream cell. For routing, the influence of

wetlands, reservoirs and lakes is taken into account. Transport between cells is assumed to occur only as surface water flow, and groundwater is assumed to return to the surface before it leaves the cell. The consumptive water use in a cell as computed by the Global Water Use Model is subtracted from the natural discharge of each cell before discharge is transported to the downstream cell. In 724 drainage basins, the Global Hydrology Model is calibrated against measured discharge by adjusting a runoff coefficient. The runoff coefficient is regionalized to the uncalibrated drainage basins based on a multiple regression analysis employing some independent basin characteristics.

#### *2.2.4.1 Vertical water balance of freshwater bodies*

The identification of the location and the extent of open inland waters (wetlands, lakes and reservoirs) is important for both the vertical water balance, due to their high evaporation, and for lateral transport, due to their retention capacity. A new global data set of wetlands, lakes and reservoirs was generated (Lehner and Döll, 2001), which is based on digital maps (ESRI, 1993 – wetlands, lakes and reservoirs; ESRI, 1992 – wetlands, lakes, reservoirs and rivers; WCMC, 1999 – lakes and wetlands; Vörösmarty et al., 1997 – reservoirs) and attribute data (ICOLD, 1998 – reservoirs; Birkett and Mason, 1995 – lakes and reservoirs). Wetlands also encompass some stretches of large rivers, as it can be assumed that only a river with adjacent wetlands (floodplain) is wide enough to be drawn as a polygon on the 1:3 million map of ESRI (1992). The data set distinguishes *local* from *global* lakes and wetlands, the local open water bodies being those that are only reached by the runoff generated within the cell and not by the discharge from the upstream cells. The data set contains the areas and locations of 1648 lakes larger than 100 km<sup>2</sup> (of which 1400 are named), and of 680 reservoirs with a storage capacity larger than 0.5 km<sup>3</sup>. Information on the storage capacity and the main purpose of the reservoirs is included. In addition, some 300 000 smaller "lakes" are taken into account, for which it could not be determined whether they are natural lakes or man-made reservoirs. In the generated data set, wetlands cover 6.6% of the global land area (without Antarctica and Greenland), and lakes and reservoirs 2.1%.

In WaterGAP, actual evaporation from open water bodies is assumed to be equal to potential evapotranspiration, and runoff is the difference between precipitation and potential evapotranspiration. In addition, potential evapotranspiration is assumed to be the same for all types of water bodies and for the land areas. In reality, wetland evapotranspiration can be lower or higher than open water evaporation, but not enough knowledge and information exists to model different evaporative behaviors. The main difference between lakes (and reservoirs) and wetlands is that the latter can fall dry, while the former are assumed to have a constant surface area from which evaporation occurs. However, the gradual changes of wetland extent during desiccation are not modeled. It is assumed that as long as there is water stored in the wetland, its area is constant; only if there is no more water left, the open water area and thus evaporation becomes zero.

### 2.2.4.2 Vertical water balance of land areas (canopy and soil water balances)

The vertical water balance of land areas is described by a canopy water balance (representing interception) and a soil water balance. The canopy water balance determines which part of the precipitation already evaporates from the canopy, and which part reaches the soil. The soil water balance partitions the incoming throughfall into actual evapotranspiration and total runoff. Finally, the total runoff from the land area is partitioned into fast surface runoff and groundwater recharge.

**Canopy water balance.** Canopy storage enables the evaporation of the precipitation before it reaches the soil. In case of a dry soil, for example, interception generally leads to increased total evapotranspiration. Interception is simulated by computing the balance of the water stored by the canopy as a function of total precipitation, throughfall and canopy evaporation. Following Deardorff (1978), canopy evaporation  $E_c$  [mm/d] is described as

$$E_c = E_{pot} \left( \frac{S_c}{S_{cmax}} \right)^{2/3} \quad (2.4)$$

with  $S_{cmax} = 0.6 \text{ mm} * LAI$ , where  $S_c$  = water stored in the canopy [mm],  $S_{cmax}$  = maximum amount of water that can be stored in the canopy [mm] and  $LAI$  = one-sided leaf area index. Daily values of the leaf area index are modeled as a function of land cover and climate. No difference is made between the interception of rain and snow.

Land cover is assumed to be homogeneous within each grid cell. The global land cover grid as modeled by IMAGE 2.1 (Alcamo et al., 1998), with 16 classes, is used.

**Soil water balance.** The soil water balance takes into account the water content of the soil within the effective root zone, the effective precipitation (the sum of throughfall and snowmelt), the actual evapotranspiration and the runoff from the land surface. Actual evapotranspiration from the soil  $E_a$  [mm/d] is computed as a function of potential evapotranspiration from the soil (the difference between the total potential evapotranspiration and the canopy evaporation), the actual soil water content in the effective root zone and the total available soil water capacity as

$$E_a = \min \left( (E_{pot} - E_c), (E_{potmax} - E_c) \frac{S_s}{S_{smax}} \right) \quad (2.5)$$

where  $E_{potmax}$  = maximum potential evapotranspiration [mm/d] (10 mm/d),  $S_s$  = soil water content within the effective root zone [mm],  $S_{smax}$  = total available soil water capacity within the effective root zone [mm]. The smaller the potential evapotranspiration from the soil, the smaller is the critical value of  $S_s/S_{smax}$  above which actual evapotranspiration equals potential

evapotranspiration.  $S_{s\max}$  is computed as the product of the total available water capacity in the uppermost meter of soil (Batjes, 1996) and the land-cover-specific rooting depth.

Following the approach of Bergström (1994), total runoff from land  $R_l$  [mm/d] is computed as

$$R_l = P_{eff} \left( \frac{S_s}{S_{s\max}} \right)^\gamma \quad (2.6)$$

where  $P_{eff}$  = effective precipitation [mm/d],  $\gamma$  = runoff coefficient (calibration parameter).

Applying a heuristic approach, total runoff is partitioned into fast surface and subsurface runoff and slow groundwater runoff (or baseflow) using information on the cell-specific slope characteristics, soil texture, hydrogeology and the occurrence of permafrost and glaciers. A detailed description of the partitioning is given in Döll et al. (2000).

#### 2.2.4.3 Lateral transport

Within a grid cell, the runoff produced in the cell and the volume of water coming from the cell upstream can be transported through a series of storages representing the groundwater, lakes, reservoirs, wetlands and the river. *Local* and *global* lakes and wetlands are distinguished, where global means that the open water units are not only recharged by local runoff but also by the discharge from upstream. Groundwater and river are treated as linear storages, lakes, reservoirs and wetlands as nonlinear storages. Then, the total cell discharge is routed along the drainage direction map to the next downstream cell. Velocity of streamflow in rivers is assumed to be 1 m/s world-wide.

#### 2.2.4.4 Subtraction of consumptive water use

River discharge (and lake storage) is affected by water withdrawals and return flows. In particular, discharge in river basins with extensive irrigation is significantly reduced by water use. In European river basins, consumptive use in 1995 amounts to, on average, 9% of the natural discharge (long-term 1961-90 average) (Kaspar et al., 2001). In the large basins of Central Europe, the value is 3-6%, in the Danube basin 9%, in the Thames basin 20% and in the Guadalquivir basin 88%. In order to be able to compare measured and computed discharges (or to calibrate the hydrological model) it is therefore necessary to consider the effect of water use in the discharge computation. In WaterGAP 2.1, the consumptive water use of each cell (calculated by the Global Water Use Model) is subtracted from the discharge that is computed as the sum of the inflow and the runoff generated within the cell. However, the computed cell-specific consumptive water use for a certain day is often larger than the cell discharge at that day, even if there is no lake or reservoir in the cell that can be used as water source. This is due to model uncertainties with respect to the computed use and discharge

values and may be also due to long-distant transport of water by canals or the effect of upstream reservoirs that cannot be modeled properly. In order to account for the latter effect, the subtraction of the consumptive use can be delayed until a wetter period (Kaspar et al., 2001); this could be interpreted as simulating withdrawals from groundwater and the effect of groundwater storage. If even over one year the consumptive use cannot be satisfied by the cell discharge, an attempt is made to cover the demand for water by subtracting it from the discharge of a neighboring cell (the cell with the largest 1961-90 long-term average discharge). In many regions of the globe, a significant part of the computed demand can still not be covered, which might be partly due to the use of nonrenewable water resources (fossil groundwater).

#### *2.2.4.5 Calibration and regionalization*

Due to the complexity of the system, the large scale and the limited quality of the input data, it is not possible to compute good discharge estimates by only using independent data sets. Therefore, the hydrological model has a small number of calibration parameters. The first step of the calibration process is the calibration of the vertical water balance. This is achieved, at least approximately, by adjusting the runoff coefficient  $\gamma$  (Equation 2.6) in the respective upstream areas (the same value is assigned to the  $\gamma$  of all cells between two discharge gauges) such that the computed long-term average annual discharge at 724 globally distributed stations (provided by the Global Runoff Data Centre GRDC, Koblenz, Germany, in 1999) is within 1% of the measured one. The minimum drainage basin size considered is 9000 km<sup>2</sup>, and the stations along a river were selected such that the inter-station areas are generally larger than 20 000 km<sup>2</sup>. The stations were co-referenced to the 0.5° drainage direction map DDM30 in order to allow the comparison between measured and computed discharges. The model was calibrated to discharge of the last thirty measurement years (or fewer years, depending on data availability). The calibration basins cover about 50% of the global land area excluding Greenland and Antarctica. The parameters describing the dynamics of lateral transport are not calibrated in WaterGAP 2.1.

To our knowledge, this is the first calibration of a global hydrological model in a large number of drainage basins. In his study of streamflow in Europe, Arnell (1999) only tuned some model parameters uniformly across Europe but did not perform a basin-specific calibration. As a result, a fifty percent error between simulated and observed long-term average discharge in large European river basins was not uncommon. In their global study, Fekete et al. (1999) combined discharge measurements with model results not by calibrating the model, i.e. by adjusting some model parameters, but by introducing a correction factor that is the ratio of modeled and measured long-term average discharge. Thus, they used the hydrological model for a spatial interpolation of long-term average runoff. They did not take into account, however, that in many river basins discharge is significantly reduced by

consumptive water use. Finally, land surface parameterizations of atmospheric models, which also compute runoff at the global scale, do not include basin-specific calibration parameters either, and, in general, computed discharges do not fit the measured ones.

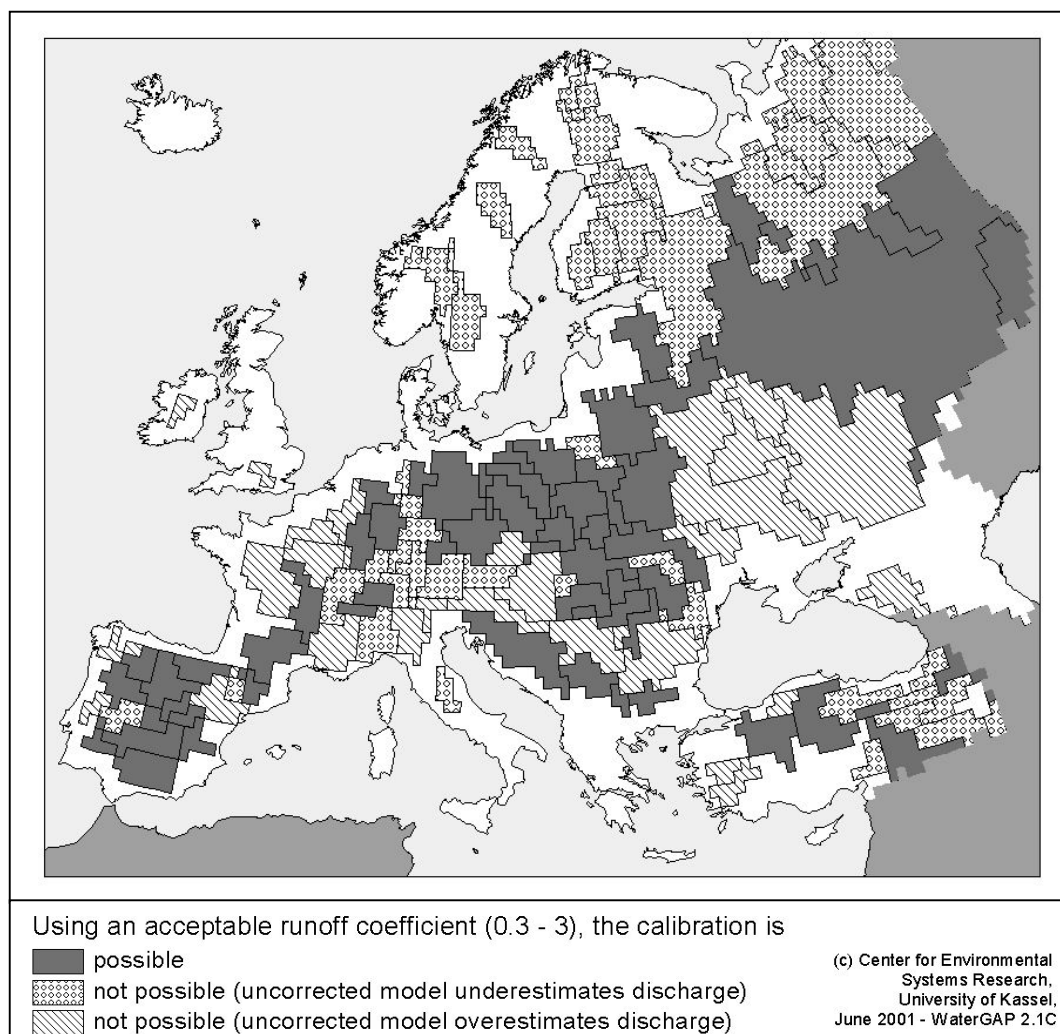
In only 327 out of the 724 calibration basins globally, the runoff coefficient  $\gamma$  was calibrated to be within physically plausible limits (between 0.3 and 3). These basins cover 27 million km<sup>2</sup>, or about 40% of the total area of the calibration basins. If  $\gamma$  is calibrated to be lower than 0.3 (in 273 basins), considerable runoff will occur even if the soil is very dry, and if it is above 3 (in 124 basins), runoff will be extremely small even well above the wilting point. Thus, a runoff coefficient outside the range of 0.3 to 3 prevents the hydrological model from simulating the soil water dynamics in a realistic manner. In the basins where the model under- or overestimates discharge even with  $\gamma$ -values of 0.3 and 3, respectively,  $\gamma$  was fixed at 0.3 or 3, and a runoff correction factor was defined as the ratio between the average of the measured discharge over the calibration period and the average computed discharge. Whenever runoff is computed in these basins, the simulated value is multiplied by the runoff correction factor to adequately represent the measured discharge values. This procedure is similar to the approach taken by Fekete et al. (1999) for all river basins. In basins where such a runoff correction factor has to be applied, the model only serves to interpolate measured discharge in space and time. The dynamics of the water cycle, however, are no longer modeled correctly and, for example, the computed evapotranspiration is not consistent with the corrected runoff estimate.

Figure 2.1 shows in which European river drainage basins (55 out of 126 calibration basins) the hydrological model could be successfully calibrated, i.e. using runoff coefficients between 0.3 and 3. In the 45 basins where the runoff coefficient was set to 0.3, the model would underestimate discharge without the introduced correction factor. This is mainly the case in snow-dominated river basins in Northern Europe and the Alps and is explained by the fact that snow precipitation is strongly underestimated by precipitation gauges. To test this hypothesis, the precipitation values of New et al. (2000), which are based on precipitation measurements and are not corrected for measurement errors, were corrected applying the monthly precipitation correction factors of Legates and Willmott (1990). According to this data set the actual precipitation is, on the global average, 11% larger than measured precipitation but up to 300% larger in snow-dominated areas. Using the corrected precipitation, the calibrated runoff coefficients of many snow-dominated river basins increase significantly, i.e. they improve. However, for a very large number of other basins, the calibrated runoff coefficients then leave the plausible range and become greater than 3. For example in some Central European basins, the Legates and Willmott precipitation correction factors appear to be too high. As no other correction factors are available at the global scale, we decided to use uncorrected precipitation.

In 26 out of the 126 European calibration basins, the model would overestimate discharge if no correction factor were applied (Figure 2.1). On the global scale, such an

overestimation often occurs in arid and semi-arid areas, and might be due to an inappropriate model formulation. In the model, for example, losses of the river e.g. to phreatophyte evapotranspiration or to the groundwater, and the evaporation from many small ephemeral ponds forming after rainfall cannot be taken into account. In river basins with large consumptive water use, a relatively small underestimation of consumptive use by the Global Water Use Model might lead to an overestimation of discharge. However, there is not yet a plausible explanation for the discharge overestimation in the European basins (e.g. in the Danube and Seine basins).

In general, the computed discharge is very sensitive to the uncertain precipitation input as well as to the potential evapotranspiration, which again depends on radiation data. Furthermore, in many regions of the globe, the evaporation of intercepted water or from lakes and wetlands, both of which are not adjusted by the calibration, form a large part of total evaporation, such that the adjustment of the runoff coefficient can often be ineffective for achieving a good fit between measured and computed discharges.



**Figure 2.1:** River basins in which WaterGAP 2.1 could be calibrated by adjusting the runoff coefficient within plausible limits (0.3 to 3).

The quality of hydrological models is often assessed by the Nash-Sutcliffe coefficient  $C_{NS}$ , which measures the efficiency of the model by relating the goodness-of-fit of the model to the variance of the measurement data (annual discharge values). If  $C_{NS}$  is larger than 0.5, the inter-annual variability of discharge is represented well by the computation, whereas if it is below zero, the variability is not captured at all. In most of Europe,  $C_{NS}$  is above 0.5 (Figure 2.2), even in many of those basins (e.g. in the Danube river basin) which could not be calibrated (see Figure 2.1). There are only very few basins that could be calibrated and still have a  $C_{NS}$  below 0.5.

Runoff coefficients in the uncalibrated river basins are regionalized using a multiple linear regression approach. The runoff coefficients of 296 selected calibration basins were found to be correlated to three basin-specific variables: a) 1961-90 average values of potential evapotranspiration, b) area of open freshwater (with wetlands at their maximum extent) as a ratio of the total catchment area, c) groundwater recharge factor (which influences the ratio of groundwater recharge to total runoff from land). An  $R^2$  of 0.53 was obtained for this regression and the derived equation was then used to determine the runoff coefficients in the uncalibrated basins.

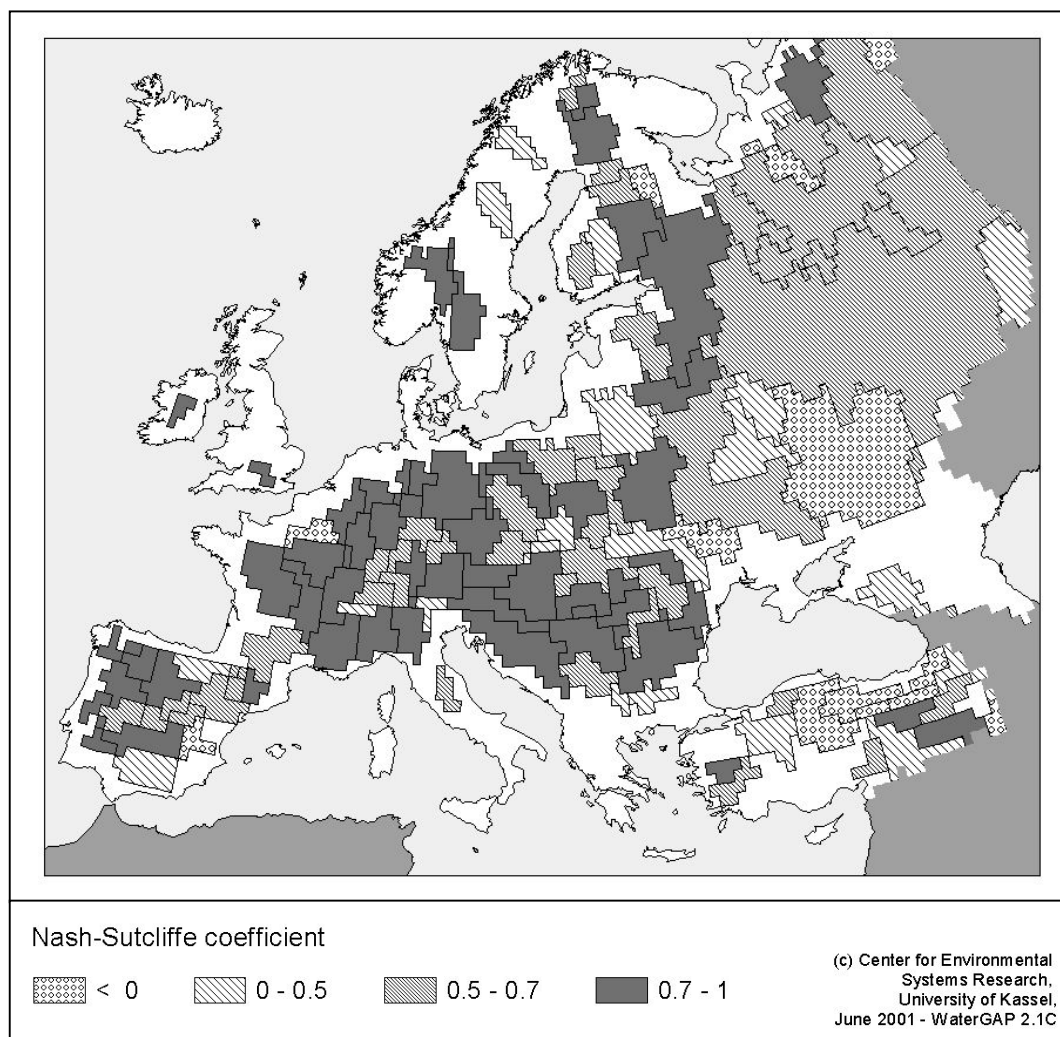


**Figure 2.2:** Nash-Sutcliffe coefficients for annual discharges in 126 calibration basins (for the calibration periods).

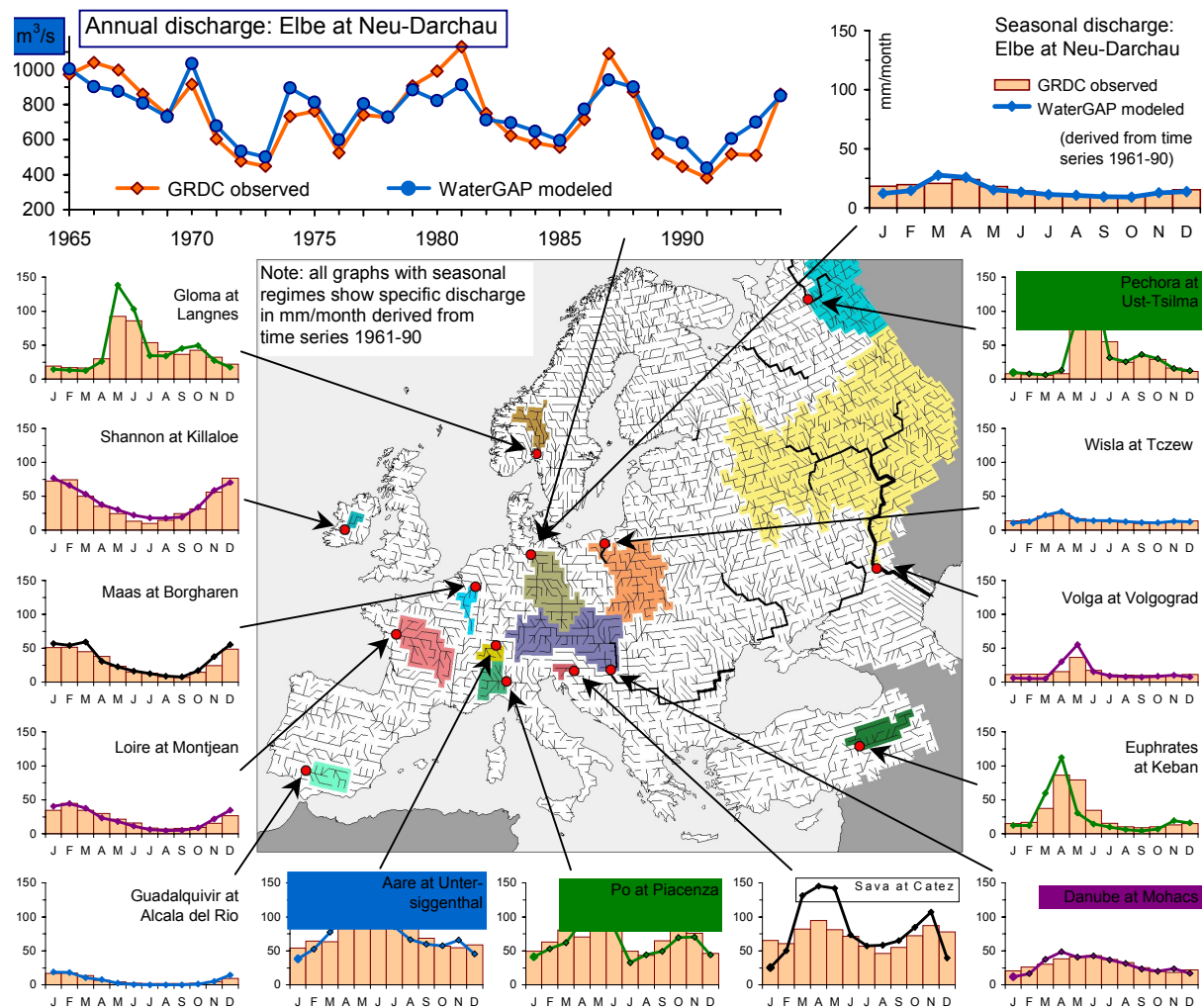


**Figure 2.3:** Comparison of observed and simulated discharge for selected European rivers (time series of annual discharge in the case of the Elbe river, long-term average 1961-90 seasonal regimes for all rivers). The colors of the lines, which indicate the seasonal discharge regime as simulated by WaterGAP 2.1, have the following meaning: Blue: In this drainage basin, WaterGAP can be calibrated by adjusting the runoff coefficient within the range of 0.3 to 3. Green: Without correction, WaterGAP would underestimate discharge. Purple: Without correction, WaterGAP would overestimate discharge. Black: Uncalibrated basin, but within a larger calibrated basin.

Figure 2.3 finally provides an overview of the performance of WaterGAP 2.1 for selected European rivers. In the upper left corner of the figure, a time series of annual discharge as computed by WaterGAP is compared to the discharge observed in the Elbe at station Neu-Darchau (the model was calibrated against discharge at this station). The inter-annual variability of discharge is represented quite reasonably by WaterGAP ( $C_{NS} = 0.77$ ). For both the Elbe river and another 13 stations throughout Europe, the computed seasonal regime (long-term average 1961-90) is compared to observed data. These stations (including the Elbe) comprise 12 basins where WaterGAP was calibrated and two uncalibrated subbasins (each located within a larger calibrated basin). Of the selected calibrated basins, four can be modeled with a runoff coefficient within the range 0.3 to 3, while for the other eight, a correction factor had to be introduced to achieve that the computed long-term average

discharge is within 1% of the observed one. The selected stations are not those with the very best results, but the selection is somewhat biased towards the positive side. For most of the selected stations, the computed seasonal regime reflects the observed one very well, independent of the need to apply a correction factor or not. This indicates that the runoff coefficient range of 0.3 to 3 is indeed a “physically plausible” range in which the dynamics of the vertical water balance are simulated well (the correction factor only serves to shift the seasonal regime curve up or down), and that even in the basins where a runoff correction is necessary the resulting monthly discharge values are satisfactory to good. The major discrepancies occur in late winter to early spring, where in many snow-dominated basins WaterGAP underestimates discharge in late winter and overestimates it in the spring; in the model, it appears that too much snow is stored during the winter and hence melting in spring occurs more accentuated than in reality. With respect to the two uncalibrated basins, the performance of WaterGAP is of different quality. The fit between simulated and observed regime is very good in the case of the Maas, where even without calibration the observed and simulated long-term average discharges are quite similar. In the case of the very small drainage basin of the Sava at Catez, it may again be the inappropriate snow modeling which causes the discharge discrepancies in winter and spring.

### 2.3 Conclusions

WaterGAP 2.1 is an integrated global water quantity model which is unique in that:

- It includes the only comprehensive global water use model which computes sectoral water uses for grid cells and drainage basins.
- It includes a global hydrological model that is calibrated against measured discharge for about 50% of the global land area.
- It is based on the best global data sets available.
- The hydrological model computes both natural and actual discharge (by taking into account discharge reduction by water use).
- The impact of climate variability on water availability and irrigation water use is taken into account.
- The important driving forces of global change are included such that relevant global change scenarios can be generated.

With respect to the quality of the model results, it is necessary to distinguish scenario generation from the ability of the model to represent present-day or historic conditions. While the quality of scenario results strongly depends on the assumed driving forces, the ability of the model to represent the historic and current situation can be described as follows: The Global Hydrology Model is able to model annual values of runoff and discharge well, while modeling of daily values is not possible (therefore, e.g. flood modeling is limited to flood statistics, see Chapter 6). The modeling of monthly discharges is certainly less reliable than

that of annual values but mostly satisfactory to good (see Figure 2.3 and the validation efforts in Chapters 3 and 7) even in river basins that require the introduction of a correction factor. A validation of the Global Irrigation Model showed a generally good correspondence to independent estimates of irrigation requirements. The domestic and industrial water use models could not be validated yet due to the lack of independent data.

In the future, basin studies will help to improve the WaterGAP model. Improvements are planned for both the Global Hydrology and the Global Water Use Model. With respect to the Global Hydrology Model, the aim is to improve the goodness-of-fit of monthly discharge values (either by calibration or by modified algorithms), e.g. by changing the method to compute potential evapotranspiration (Penman-Monteith vs. Priestley-Taylor), by modifying the snow module (timing of snowmelt, floods) and by improving the precipitation correction and groundwater recharge estimation. With respect to irrigation water use, the map of irrigated areas will be continually improved in cooperation with FAO, and it is planned to consider the impact of permanent crops on irrigation water use. Industrial water use modeling will become more realistic when water use by thermal power plants is explicitly simulated. Further improvements of the Global Water Use Model will depend on the availability of new high-quality data.

## 2.4 References

- Alcamo, J., Döll, P., Henrichs, T., Kaspar, F., Lehner, B., Rösch, T., Siebert, S. (2001): WaterGAP 2: A model for global assessment of freshwater resources. (submitted to Hydrological Sciences Journal).
- Alcamo J, Henrichs T, Rösch T (2000): World Water in 2025 - Global modeling and scenario analysis. In: Rijsberman F (ed): World Water Scenarios – Analyses. Earthscan Publications, London.
- Alcamo, J., Leemans, R.; Kreileman, E. (eds) (1998): Global Change Scenarios of the 21st Century. Results of the IMAGE 2.1 Model. Pergamon.
- Arnell, N.W. (1999): A simple water balance model for the simulation of streamflow over a large geographic domain. *J. Hydrol.* 217, 314-335.
- Batjes, N.H. (1996): Development of a world data set of soil water retention properties using pedotransfer rules. *Geoderma*, 71, 31-52.
- Bergström, S. (1994): The HBV model. In V.P. Singh (ed): Computer Models of Watershed Hydrology. Water Resources Publications: 443-476.
- Birkett, C.M., Mason, I.M. (1995): A new global lakes database for a remote sensing programme studying climatically sensitive large lakes. *Journal of Great Lakes Research*, 21(3), 307-318.
- Deardorff, J. W. (1978): Efficient prediction of ground surface temperature and moisture, with inclusion of a layer of vegetation. *J. Geophys. Res.*, 86C, 1889-1903.
- Döll, P., Kaspar, F., Lehner, B. (2001): A calibrated hydrological model for deriving water availability indicators. (submitted to *J. Hydrol.*).
- Döll, P., Lehner, B. (2001): Validation of a new global 30-min drainage direction map. (*J. Hydrol.*, accepted).
- Döll, P., Siebert, S. (2001): Global modeling of irrigation water requirements. (*Water Resour. Res.*, accepted).
- Döll, P., Siebert, S. (2000): A digital global map of irrigated areas. *ICID Journal*, 49(2), 55-66.
- Döll, P., Lehner, B., Kaspar, F. (2000): Global modeling of groundwater recharge and surface runoff. *EcoRegio* 8, Geographisches Institut der Universität Göttingen, 73-80.
- Döll, P., Kaspar, F., Alcamo, J. (1999): Computation of global water availability and water use at the scale of large drainage basins. *Mathematische Geologie*, 4, 111-118.

- ESRI (1993): Digital Chart of the World 1:1 M.
- ESRI (1992): ArcWorld 1:3 M Continental Coverage.
- FAO (1995): Digital Soil Map of the World and Derived Soil Properties, CD-ROM Version 3.5, FAO, Rome.
- Fekete, B.M., Vörösmarty, C.J. & Grabs, W. (1999): Global composite runoff fields of observed river discharge and simulated water balances. Report No. 22, Global Runoff Data Centre, Koblenz, Germany.
- Forsythe, W.C., E.J. Rykiel, R.S. Stahl, H. Wu, Schoolfield, R.M. (1995): A model comparison for daylength as a function of latitude and day of year, *Ecol. Modelling*, 80, 87-95.
- Geng, S., F.W.T. Penning, Supit, I. (1986): A simple method for generating daily rainfall data, *Agric. For. Meteor.* 36, 363-376.
- GlobalARC GIS Database (1996): by CRSSA, Rutgers University and U.S. Army CERL.
- ICOLD (International Commission on Large Dams) (1998): Word Register of Dams (CD-ROM), Paris, France.
- Kaspar, F., Döll, P., Lehner, B. (2001): Globale Modellierung der Durchflussverminderung durch konsumptive Wassernutzung. In: Suttmöller, J., Raschke, E.: Modellierung in meso-bis makroskaligen Flußeinzugsgebieten – Tagungsband zum gleichnamigen Workshop am 16./17. November 2000 in Lauenburg, GKSS 2001/15, GKSS Geesthacht.
- Legates, D.R. & Willmott, C.J. (1990): Mean seasonal and spatial variability in gauge-corrected, global precipitation. *Int. J. Climatology* 10, 111-117.
- Lehner, B., Döll, P. (2001): WELAREM1 - A global lakes, reservoirs and wetlands data set. Data set description sheet, Center for Environmental Systems Research, University of Kassel, Germany.
- New, M., Hulme, M., Jones, P.D (2000): Representing twentieth century space-time climate variability. Part II: Development of 1901-96 monthly grids of terrestrial surface climate. *J. Climate* 13, 2217-2238.
- Priestley, C., Taylor, R. (1972): On the assessment of surface heat flux and evaporation using large scale parameters, *Mon. Weather Rev.* 100, 81-92.
- Roth, D. (1993): Richtwerte für den Zusatzwasserbedarf in der Feldberegnung, Schriftenreihe der LUFA Thüringen, 6, 53-86.
- Shuttleworth, W.J. (1993): Evaporation. In Maidment, D.R. (ed): *Handbook of Hydrology*, pp. 4.1 - 4.53, McGrawHill.
- Shiklomanov, I. (2000): World water resources and water use: Present assessment and outlook for 2025 (supplemented by CD-ROM: Shiklomanov, I., World freshwater resources, available from: International Hydrological Programme, UNESCO, Paris), in Rijsberman, F.R. (ed.): *World Water Scenarios: Analysing Global Water Resources and Use*, Earthscan Publications, London.
- Siebert, S., Döll, P. (2001): A Digital Global Map of Irrigated Areas – An Update for Latin America and Europe. *World Water Series 4*, Center for Environmental Systems Research, University of Kassel, Germany.
- Smith, M. (1992): CROPWAT - A computer program for irrigation planning and management, *FAO Irrigation and Drainage Paper*, 46, Rome, Italy.
- Solley, W.B., R.S. Pierce, Perlman, H.A. (1998): Estimated use of water in the United States in 1995, USGS Circular 1200. <http://water.usgs.gov/public/watuse/>.
- USGS (United States Geological Survey) (2000): HYDRO1k. <http://edcdaac.usgs.gov/topo30/hydro/>.
- van Woerden, J. W., Diederiks, J., Goldewijk, K.Klein (1995): Data Management in Support of Integrated Environmental Assessment and Modelling at RIVM - Including the 1995 RIVM Catalogue of International Data Sets . RIVM Report No. 402001006.
- Vörösmarty, C.J., Sharma, K., Fekete, B., Copeland, A.H., Holden, J., Marble, J., Lough, J.A. (1997): The storage and aging of continental runoff in large reservoir systems of the world. *Ambio*, 26: 210-219.
- World Bank (1996): *World Development Report 1996*. Oxford University Press.
- WCMC (World Conservation Monitoring Centre) (1999): *Wetlands Dataset*, Cambridge, UK.
- WRI (World Resources Institute) (1998): *World Resources 1998-99*, Oxford University Press, New York, USA.